Estuarine, Coastal and Shelf Science 291 (2023) 108438

Contents lists available at ScienceDirect

Estuarine, Coastal and Shelf Science

journal homepage: www.elsevier.com/locate/ecss

Assessing benthic marine habitats colonized with *posidonia oceanica* using autonomous marine robots and deep learning: A Eurofleets campaign

Miquel Massot-Campos [a,*], Francisco Bonin-Font [b], Eric Guerrero-Font [b], Antoni Martorell-Torres [b], Miguel Martin Abadal [b], Caterina Muntaner-Gonzalez [b], Bo Miquel Nordfeldt-Fiol [b], Gabriel Oliver-Codina [b], Jose Cappelletto [a], Blair Thornton [a,c]

[a] *Centre of Excellence for In situ and Remote Intelligent Sensing, University of Southampton, Southampton, SO16 7QF, Hampshire, United Kingdom*
[b] *Systems, Robotics and Vision, University of the Balearic Islands, ctra de Valldemossa, km 7.5, Palma de Mallorca, 07122, Balearic Islands, Spain*
[c] *Institude of Industrial Science, University of Tokyo, 4-chōme-6-1 Komaba, Meguro, 153-8505, Tokyo, Japan*

ARTICLE INFO

Dataset link: https://www.emodnet-ingestion.eu/submissions/submissions_details.php?menu=39&tpd=1051&step_more=12_14_17&step=0821

Keywords:
Assessment of marine ecosystems
Seagrass
Autonomous marine vehicles
Lagrangian drifters
Computer vision
Convolutional neural networks

ABSTRACT

This paper presents a methodology for observing and analyzing marine ecosystems using images gathered from autonomous marine vehicles. Visual data is composed in photo-mosaics and classified using machine learning algorithms. The approach expands existing solutions, enabling extended monitoring in time, space, and depth. Imagery was collected during a field campaign in the Spanish marine and terrestrial protected area of Cabrera, Balearic Islands, colonized by the endemic seagrass species *Posidonia oceanica* (*Po*). The operations were performed using three distinct platforms, an *Autonomous Underwater Vehicle* (AUV), an *Autonomous Surface Vehicle* (ASV) and a *Lagrangian Drifter* (LD).

Results are compared to prior habitat maps to assess seagrass meadow distribution. The proposed solution can be scaled and adapted to other locations and species, considering limitations in data storage and battery endurance.

1. Introduction

Posidonia oceanica (*Po*) is a seagrass endemic to the Mediterranean with a high ecosystemic value, as it absorbs carbon and releases oxygen, provides habitats to numerous marine species, stabilizes the seabed, and increases seafloor roughness, breaking swell and wind-driven waves and encouraging the deposit of sedimentary particles (Piñeiro-Juncal et al., 2021). *Po* also acts as a host to filterers, such as sponges, and provides the surrounding ecosystems with oxygenated waters. This plant is also an excellent bioindicator: since, a) it is very sensitive to physical impacts (DiCarlo, 2004) and environmental stressors, such as the presence of pollutants, rising temperatures or salinity variations (Bonanno and Martino, 2017), and b) it is a long-lasting species: it has a slow growth rate (1–6 cm of rhizome per year) and a very slow natural recolonization rate, lasting up to decades to recover original extensions after significant damage (Marbà and Duarte, 1998). *Posidonia* habitat range extends from the shore down to approximately 50-meter depth being able to survive only with indirect light. Despite its importance for marine ecosystems, this species is in a vulnerable situation, suffering a clear regression in the last few years (Fabio et al., 2022). The main causes of its regression are anthropogenic: leisure anchoring, sewage outflows or accidental spills, fish farms, or climate change, among others (Marbà and Duarte, 2010; Kiparissis et al., 2011; Deter et al., 2017; Bonin-Font et al., 2018; Abadie et al., 2018). However, the situation can be potentially rectifiable with ambitious plans for monitoring and controlling at a local scale, which can inspire the subsequent correction and regeneration actions (Fabio et al., 2022). *Posidonia* meadows have been recognized by the European Council as habitats of special control and protection, which is reflected in several directives such as the European Union Habitat Directive 92/43/EEC related to the areas included in the Natura 2000 Network (European Commission, 2008b), and by the Marine Strategy Framework Directive 2008/56/EC (European Commission, 2008a).

The biological indicators used to assess the state of *Po* are often its upper and lower limits, leaves and bulbs density and bottom coverage (Sylvie et al., 2009). Typical approaches to measure the extent of the meadows use the Line Intercept Transects (LIT) strategy (Gambi et al., 2004). LIT requires divers to hammer a stake into the seafloor, at the rough center of a meadow. Then, they extend measuring tape

* Corresponding author.
Linkedin: miquelmassot (M. Massot-Campos).
E-mail addresses: miquel.massot-campos@soton.ac.uk (M. Massot-Campos), francisco.bonin@uib.es (F. Bonin-Font).

https://doi.org/10.1016/j.ecss.2023.108438
Received 22 January 2023; Accepted 14 July 2023
Available online 20 July 2023

in multiple directions and annotate the lengths up to the border of the meadow (Fernández-Torquemada et al., 2020). These sparse in situ measurements are extrapolated to the whole patch to compute its surface. Density is estimated using *quadrat* frames at random sampling locations. Divers then count the number of leaves and bulbs within the frame (McKenzie, 2003). Due to the limited capacity of air tanks, safety of divers and ship logistics, this approach often requires multiple immersions to cover an extensive habitat. These methods heavily rely on human intervention, delivering a few field observations per dive and result in a large uncertainty, especially in zones with a patchy cover.

Fig. 1-(a) shows the *in situ* deployment of a quadrat frame used to measure the density of seagrass leaves. Figs. 1-(b) to 1-(d) show three samples of quadrat frames pictured *in situ*, with more density of leaves in (b) and (d) and with less density in (c). The side size of frames ranges between 30 and 70 centimeters, approximately. The difference in colors and tonalities between pictures (b), (c) and (d) is another bio-indicator of the state of the plant and the season. Figs. 1-(e)–(f) show the deployment of the stripes to measure coverage in an area densely colonized with *Po*. All pictures were taken during real campaigns in the context of the DETECPOS (UIB and IMEDEA, 2022) project, in which the Systems, Robotics and Vision group of the UIB has an active role. Picture 1-(a) is courtesy of Acció Climàtica-GenCat GENCAT (2022), and Picture 1-(b) to (f) are courtesy of the Ecology and Marine Resources group, from the Mediterranean Institute for Advanced Studies (IMEDEA-UIB).

Innovation in this field is mainly focused on: (a) increasing the amount of data to be collected, broadening the spatial and temporal extension of missions and depths, while reducing or eliminating risks for humans, (b) increasing the accuracy in the *Po* range and coverage estimates, acquiring global measurements instead of partial approximations, and (c) automating the data gathering processes and ensuring accurate georeferencing of missions to enable site monitoring.

Traditional techniques involving divers are being progressively replaced by innovative robots, Artificial Intelligence (AI) and digital image processing, with ample opportunities for improvement remaining. Some primary approaches explored the use of visual or acoustic trackers to get seafloor information. Sensors were towed by divers and georeferenced using static buoys acting as a long baseline (Sgorbini et al., 2002). Other researchers discriminated different types of seafloor leveraging the sediments hyper-reflectance property (Louchard et al., 2003) or combining acoustics with imagery taken from cameras attached to boats and/or from satellites (Lemenkova, 2011). Multi-rotor aerial drones flying above the sea surface have been also used to build photo-mosaics on certain marine habitats colonized either by *Zostera noltii* or *Posidonia oceanica* (Ventura et al., 2018; Duffy et al., 2018). However, satellite or aerial imagery is not taken *in situ* but remotely, that is, far from the sources of information, which are mainly on the seafloor. In this case, the lack of details due to the water turbidity and/or the height of the water column that blurs or directly hides meadow limits and imposes additional underwater image gathering or post-processing procedures that complicate and slow down the whole system (Zoffoli et al., 2014).

Recently, *in situ* data gathering approaches have gained priority over solutions based on remote sensing. For example, Barcelona et al. (2021) mapped and analyzed meadows of *Po* through video transects recorded by a scuba diver with a GoPro camera, swimming at 2 m above the seafloor. Images of video sequences were used to build photomosaics to obtain seascapes of the explored habitats, offering a direct view of the whole inspected environment to scientists. However, this approach depends on the continuous attention of specialized personnel onboard a support vessel and neither the images nor the final mosaics were georeferenced. Acoustic bathymetry from surface vessels, occasionally combined with aerial images or visual data from an *Autonomous Surface Vehicle* (ASV), approximate better to the concept of *in situ* automated data gathering systems for seagrass georeferencing and control (Gumusay et al., 2019; Rende et al., 2020). However, actual high-quality *in situ* observations over arbitrary extents and durations, and without any risk to humans, can only be acquired by underwater robots.

The literature is scarce in approaches focused on the use of marine underwater robots to monitor and control *Po in situ*. Bathymetry with multibeam sonars (Gumusay et al., 2019) or 3D reconstructions composed combining sonar data and images (Ferretti et al., 2017; Risio et al., 2018) are some examples of early relevant work performed with *Remotely Operated Vehicles* (ROVs). However, missions with ROVs (especially at medium/high depths) usually require or imply (McLean et al., 2020): a) expensive robots and/or support infrastructures (cranes, support vessels), b) complex deployment procedures, c) permanent tethers to supply energy and pilot it, limiting its maneuverability, d) although ROVs with the right setup can be run to follow closed loop trajectories, tethers and surface vessels are still needed to managed the whole infrastructure, and trusting the shape and extent of missions to the skills of the operator is the most usual situation.

On the contrary, lightweight AUVs (Carreras et al., 2018; Ocean Scan Marine Systems and Technology Lda, 2022; Hong et al., 2017) present several advantages with respect to ROVs for *in situ* data collection: (1) they can operate in shallow areas if they are deployed from a pier (unusual in ROVs used for biological applications), (2) increased autonomy: AUVs can be pre-programmed to perform repeatable and structured trajectories at the desired depth and distance to the bottom, and, (3) its range is not limited by a tether. Contrary to ROVs, transmitting real-time data is a challenge for AUVs. Underwater wireless communications are limited to long-range, low-speed acoustics or close-range, high-speed optical links, if available. Their operation needs to be robust to communication intermittency and low-to-none data transmission during an AUV mission.

Global Positioning Systems (GPS) on these platforms enable them to geo-localize captured data. Even if GPS signal is not available underwater, localization methods that use available onboard sensors and motion models are used to estimate its trajectory.

Some authors claim that underwater image recording with single or camera arrays towed by support small boats increase performance and efficiency and reduce costs of missions with respect to systems based on ROVs or AUVS (Mizuno et al., 2020). However, trajectories cannot be pre-programmed and the motion of the cameras is subject to the boat performance, the underwater currents and the depth at which they are deployed, being its local drift hardly to control. These operations cannot be automatized unless the boat and the camera array are also robotized.

In consequence, in the last years, AUVs equipped with cameras have gained ground in applications related to marine ecology, such as fauna monitoring (Perkins et al., 2015; Verfuss et al., 2019) and the control of benthos or biomass of special interest (Williams et al., 2012; Lambertini et al., 2021; Perkins et al., 2016; Thornton et al., 2021). Occasionally, AUVs with cameras participate in teams of coordinated autonomous robotic infrastructures for deep-sea observation, including crawlers, UAVs and Gliders (Wenzhoefer et al., 2016). Now, the intention was to adapt the aforementioned previous methodologies based on autonomous vehicles to the particular case of protected Mediterranean seagrass habitats located at depths still not covered either by divers or ROVs, adding the novelty of *Convolutional Neural Networks* (CNN) for seagrass coverage computation.

Very few work has been focused specifically on applying this type of technology to get ecological variables that reflect the state of ecosystems developed on *Po*. A preliminary approach (Vasilijevic et al., 2014) included the identification of the meadow limits (upper and lower) by means of aerial photography and a side scan sonar installed on a *Lightweight AUV* (LAUV) (Ocean Scan Marine Systems and Technology Lda, 2022). In this case, the presence or absence of seagrass in selected geolocalized points is determined with image processing techniques, image by image. The coverage is estimated combining the seagrass data identified automatically in the images taken in the water, the output of the side scan sonar and the upper border of the meadows delimited

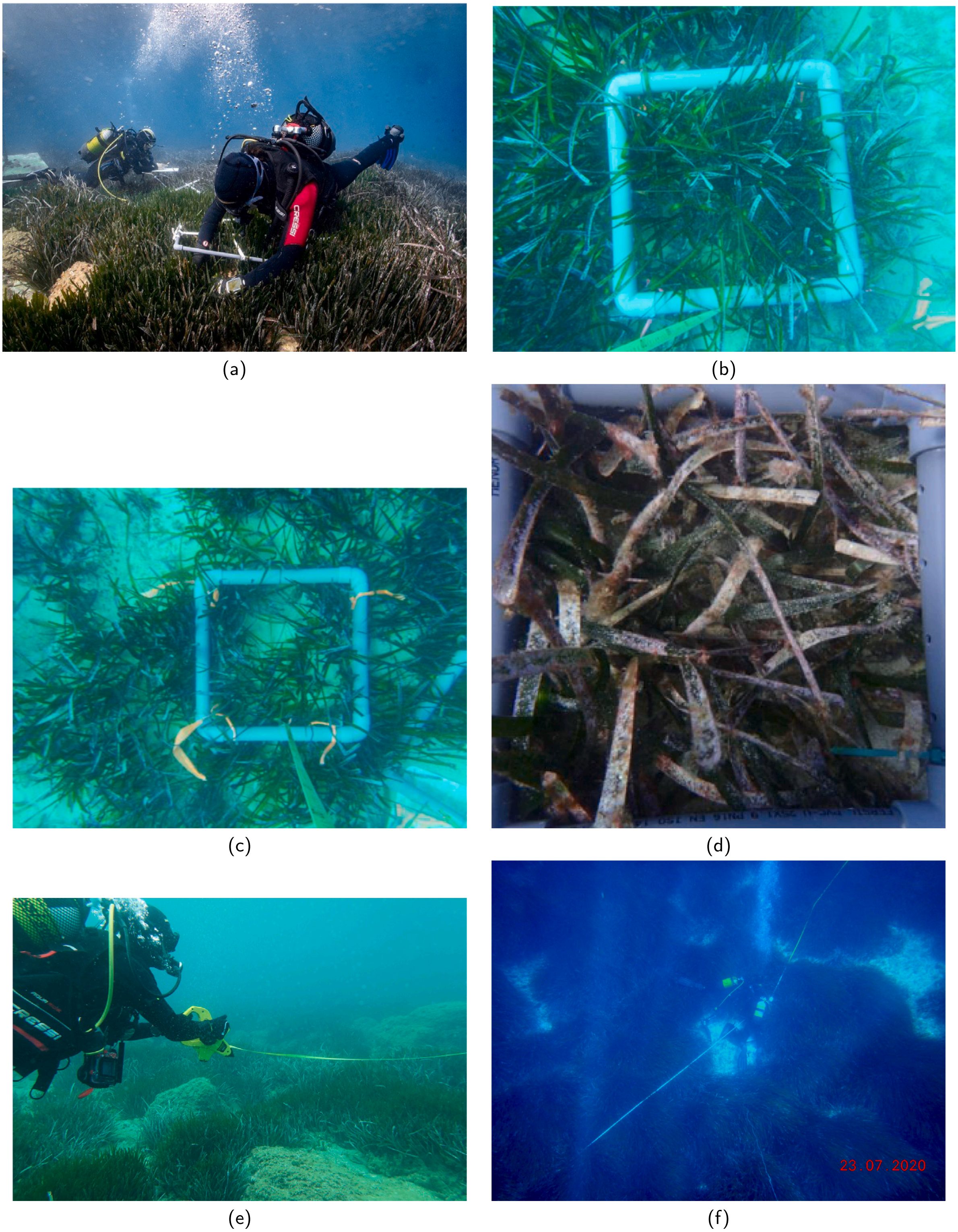

Fig. 1. (a)–(d) Quadrats. (e)–(f) Longitudinal transects.

from the aerial images. Additionally, coverage of spaces with no data is obtained by means of interpolation.

Underwater imaging provides higher spatial resolution compared to acoustic mapping. Although affected by light absorption in water and turbidity, images can be color corrected and are easy to interpret by non-expert users.

Tight collaboration between engineers and biologists has permitted to reach solutions that combine AUVs equipped with cameras to get images *in situ* with the application of *Machine Learning* (Bonin-Font et al., 2017) or *Convolutional Neural Networks* (Martin-Abadal et al., 2018) to discriminate, automatically, the seagrass from the background. The process includes several general phases, namely: (1) areas of special interest are selected and surveyed by the AUV, grabbing geo-localized images during the whole mission, (2) images from each mission are

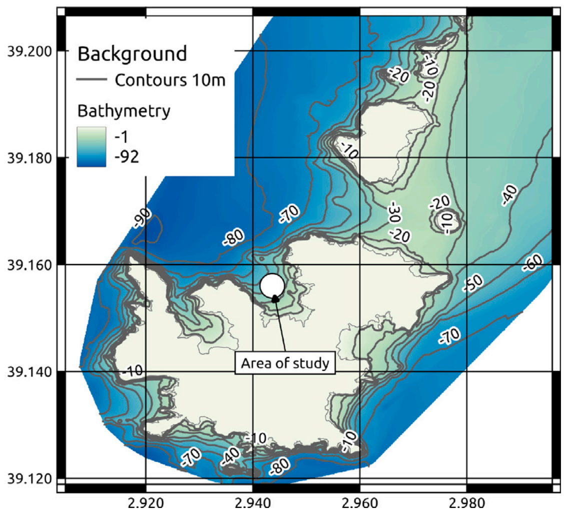

Fig. 2. Study area for GRASSMAP cruise off the coast of Cabrera MPA, between 10 and 45 meters depth.

segmented to differentiate *Po* from the rest, (3) geo-referenced photomosaics with the original colored images and with the segmented images are build as two different types of visual maps of the entire zone, (4) bottom coverage is computed by means of accounting for pixels of different gray levels in the segmented mosaic. The accuracy in the calculation of the coverage depends entirely in the performance of the different methods used to segment the seagrass, which, in the case of the CNN described in Martin-Abadal et al. (2018), precision reaches values of 96% and accuracy 97% . The methodology involves running this process throughout several yearly seasons to monitor the evolution of meadows in certain selected areas (González et al., 2021). Nonetheless, in all these described approaches, the scale of interpretation is limited to the size of the pre-programmed missions, and non-negligible latency (days, weeks, months) is introduced when generating numerical summaries due to the delay in the data post-processing procedures. A solution to overcome this is presented in Guerrero-Font et al. (2021), Guerrero et al. (2021) with adaptive replanning, conditioning online the trajectory of the AUV to the shape of the seagrass meadows observed continuously on the bottom, and using stochastic processes to model its spatial distribution .

Although all these techniques still do not form a mature technology field, they have the potential to address all the requirements needed to complete marine surveys on areas with seagrass, with an elevated degree of automation, success and accuracy. All in all, some crucial points still opened include: (1) considering the need of simpler and cheaper deployment infrastructures, (2) geo-referencing the grabbed images during the whole trajectory, (3) increasing range of missions in extension and depth up to the lower limits of meadows, (4) decreasing latency in the process and evaluation of the data gathered *in situ*, or (5) augmenting the accuracy in the computation of variables of ecological interest.

This paper presents the methodology and results of a field campaign performed during the scientific cruise GRASSMAP (Campos et al., 2021), funded by the Eurofleets+ framework, to survey and analyze areas of special ecological interest colonized with *Po*. The campaign integrated advanced robotic technology and image processing techniques and it was designed as: a) an extension of previous attempts to apply marine autonomous robots to assess benthic habitats, but now applied specifically to areas with *Po* seagrass and, b) as an expansion of previous projects and exercises described above (Vasilijevic et al., 2014; González et al., 2021), but selecting the location of the biotic areas to inspect in the basis of pre-existing biological information. Complexity, extent (in time, space and depth) and typology of the missions was enhanced thanks to the services given by the field platforms. Data collection missions were performed in the maritime domain of the Cabrera Marine-Terrestrial National Park, in zones located at depths between 20 and 45 meters and validated through comparison with an established baseline. The joint application of all the technologies involved goes one step beyond the solutions already existing in the literature addressed to inspect submarine areas with seagrass, in 6 main aspects: (1) This campaign discarded using either ROVs, due to the costs and complexity of support infrastructures needed to move and deploy this kind of robots at these depths and the impossibility to assure missions with the shape and extension needed, or aerial drones with cameras since they would be useless to detect lower limits of meadows in the selected sites, (2) the facility to explore and get data near the sea bottom with 2 different robots: one lightweight AUV and a LD, in extensive areas, at depths where operating with divers is very difficult or not recommended, and for periods of time much longer than the regular immersions, (3) perform daily analysis of inspected areas, reducing latency in the field data processing and permitting to get early conclusions about the appearance and state of the involved ecosystems, (4) the automation of the *Po* coverage estimation with mosaics and image segmentation algorithms, getting results more accurate than those obtained with traditional methods based on divers, (5) the option to geo-localize the missions and the data very accurately, and (6) the capacity to complement all the information grabbed from the different robots to get richer datasets that cover different and diverse aspects of the environment from different perspectives.

The procedures and lessons learned during the campaign could be easily transferred to the detection, assessment and coverage estimation of other species of interest, by building mosaics and 3D structures from adapted viewpoints and adjusting the models to new objectives.

2. Materials and methods

The operations were performed in a marine protected area (MPA) of the Cabrera archipelago. The area was selected due to prior habitat studies being already available. The islands are located at the south of Mallorca, in the Mediterranean Sea, and are part of the Balearic Islands. Fig. 2 shows the georeferenced location. The study was conducted at Cala Santa Maria (CSM) (lat: 39.156896, lon: 2.939445), a northern-faced bay with roughly known *Po* cover at depths ranging from 20 to 50 m. The area was selected due to (1) the low human impact, as anchoring and leisure maritime traffic are not permitted in the MPA waters, providing a representative baseline for an undisturbed location, (2) at these depths, the application of the Intercept Transects strategy would be, in general, unfeasible to get information of several hundreds of squared meters, and, (3) their strategic geo-location in the park and the availability of previous data of *Po* meadows; CSM was previously studied by divers and surveyed using an Uncrewed Aerial Vehicle (UAV) in shallow water areas (< 2 m), and its *habitat map* has been published in Marbà et al. (2002)

The aforementioned map will be used as a baseline to assess, up to a certain extent, the *Po* detection results presented in this paper. In general, there is no reliable ground truth information about *Po* coverage in the Balearic islands, which makes trusting or evaluating our results a real challenge. Nevertheless, despite the temporal difference between this baseline and the datasets obtained in this campaign, this is the unique public information available to be qualitatively compared with our output. Updates of these kind of data are not performed very often, given the slow advance of *Po* meadows and the difficulty and cost of doing immersions at the particular sites included in this work.

The case study presented in this paper was performed during the GRASSMAP Eurofleets+ campaign (Campos et al., 2021), lasting one week aboard the RV SOCIB scientific vessel (Balearic Islands Coastal Observing and Forecasting System, 2021). This is a dual-hull catamaran with a capacity for up to 7 researchers, a complete laboratory and

Fig. 3. Marine infrastructure used in this study: R/V Socib (top left), Xiroi ASV (bottom left), Floaty LD (top right) and Turbot AUV (bottom right).

all the necessary equipment to deploy and recover marine platforms, including an A-frame crane.

The data collection was performed by 3 low-cost autonomous robots: (1) a Lagrangian Drifter named *Floaty McFloatface* (Yang et al., 2020), developed by the University of Southampton, (2) a Sparus II AUV named *Turbot* (Carreras et al., 2018), manufactured by IQUA Robotics (IQUA ROBOTICS, 2022) property of the UIB and managed by the SRV Group, and (3) a surface catamaran-shaped ASV called *Xiroi* (Martorell-Torres et al., 2018), developed by the same SRV Group and with the capacity to navigate coordinately with the AUV. Fig. 3 shows a view of the vessel and the marine platforms. These 3 platforms differ in the way they operate and the amount of required human support: the Lagrangian float drifts with sea currents whilst keeping at a constant altitude from the seafloor with no further interaction with any central station until it emerges, the AUV needs a pre-defined trajectory and often relies on external global localization sensors to successfully achieve its mission with confidence (GPS and/or *Ultra Short Acoustic Baselines* (USBL)). In this campaign, the USBL head was mounted on the ASV Xiroi. Xiroi has the capacity to follow the AUV at a distance, and to communicate continuously with the support vessel via a radio frequency antenna. This wireless link is used to supervise the AUV activity and transmit critical data in short burst, but not entire images. The AUV was in charge of exploring the selected areas at approximately 3 meters from the ground following pre-programmed missions and grabbing an images every two seconds. On the other hand, the Lagrangian Drifter does not rely on a support vessel to carry out its mission. Its main purpose was to grab images as it drifted and sending selected information through globally available satellite communication bandwidths (Iridium) to a ground station, as soon as it reached the water surface.

2.1. Turbot AUV and Xiroi ASV

Turbot is a 200-meter rated, 1.6 m long, 32 cm diameter torpedo-shaped AUV, manufactured by IQUA Robotics (Carreras et al., 2018) and upgraded with vision and navigation capabilities by the University of the Balearic Islands. It has 2 surge and 1 heave propeller, 8 h of autonomy and it weighs 60 kg. The AUV is equipped with a pressure sensor, a stereo rig formed by two downwards-looking cameras with their lens axis perpendicular to the longitudinal vehicle axis, a global positioning system (GPS) to be geo-referenced when it is in the surface, a Doppler velocity log (DVL) (which outputs velocity and altitude), an inertial measurement unit (IMU) (acceleration and angular velocity), an acoustic modem which can communicate with an acoustic ultra-short baseline (USBL) head (it provides absolute position), an eco-sounder probe also pointing towards to the sea bottom and finally, two led lights. Its control architecture is based on ROS (Stanford Artificial Intelligence Laboratory et al., 2021). The self-localization module consists in a double EKF filter that integrates the data obtained from all sensors (pressure, DVL, IMU and also the USBL) and contains in its state vector, the global position (with respect the origin of the mission) and the lineal and angular velocities, with their respective covariances (Font et al., 2017). Due to the low bandwidth of the acoustic modem (13Kbps aprox.), the data exchange between the vehicle and the USBL head has to be restricted to short streams. The possibility to repeat the same trajectory at the same location, as many times as needed, is very important to get temporal series of data that permit to evaluate the evolution of a certain ecosystem in several seasons

2.2. Xiroi ASV

Xiroi ASV is a 1.6 m long and 1.2 m wide autonomous double-hull catamaran developed at the SRV group of the UIB. It is driven by two differential propellers and has an autonomy of 12 h. For navigation purposes, it is equipped with a GPS and an IMU. As payload, the ASV is equipped with a high frequency radio communications antenna and an USBL modem head hung from a pole between the two hulls at a depth of 1.5 m. In this campaign, the main purpose of the ASV was to be an acoustic communications gateway between the AUV and the central station located in the vessel. To this end, the ASV navigated coordinately with Turbot, running a *path following* behavior keeping a constant distance to the AUV. This distance was set in order to avoid common localization problems with acoustics such as multi-path (Baktash et al., 2015) and the loss of robustness and quality in the communication channel as the distance between the mobile modem and the static head increases. Data sent in the two directions, that is, from the AUV to the vessel and from the vessel to the AUV passed through the ASV, via the acoustic link between the ASV and the AUV and the radio link between the ASV and the support vessel. As the acoustic baseline is the most restrictive in terms of bandwidth, data to be transmitted among the 3 partners (AUV, ASV and vessel) were restricted to alarms or urgent notifications and services to be executed, sent from the central station to the robot. The presence of the ASV also permits to increase the distance range of communications between AUV and the support vessel. If the USBL head is installed in the vessel, the communication distance is restricted to the maximum range of this acoustic link. With the ASV, the communications can be extended to the range of the radio antenna plus the range of the USBL.

Xiroi control architecture is also based on ROS and explained with detail in Martorell-Torres et al. (2018).

2.3. Floaty LD

Floaty McFloatface is a *Lagrangian* imaging float (or Lagrangian Drifter, LD) designed and built by the University of Southampton (Yang et al., 2020). It is equipped with downward-looking stereo cameras, strobe lighting and vertical actuators to keep altitude between 2 to 4 meters. LDs are an attractive option for region-scale imaging surveys. Their operational costs are lower than AUVs, as they do not need expensive or sophisticated self-localization sensors. Drifters are more energy efficient than conventional AUVs because they do no propel themselves laterally. Instead, they passively drift on underwater currents whilst gathering images of the sea bottom. They enable missions longer than missions with AUVs (in the order of weeks). On the contrary, the drifter is incapable of precise trajectory following or repeating a survey.

Floaty can be deployed from a support vessel using winch or crane systems, and no human intervention is required during its mission. The platform is a $1 \times 0.85 \times 0.34$ m box-shaped structure with 2 heave propellers and 10 days of autonomy. It weighs 70 kg, and it is equipped with an IMU, a pressure sensor and an altimeter. In terms of safety, it uses an Iridium modem with a secondary battery, trickle-charged by the main 2 kWh lithium-ion battery. In the event of a power loss, the platform will return to the surface due to its inherent positive buoyancy. This passive safety feature will allow the Iridium modem to broadcast its position to a predefined telephone or email address for up to a year long. This allows any vessel of opportunity to recover the drifter, removing the dependence on a mother ship during its mission.

It is worth mentioning that, although *Floaty* performs semi structured surveys, which implies that, the Drifter has no control or previous knowledge of its upcoming trajectory and its planned end, seawater currents speeds and directions can be obtained using forecast data, available at Copernicus Marine Service (European Union's Earth Observation Programme, 2021), and estimating its deployment and surface location given one or more points of interest is possible, as explained in Yang et al. (2020). The Drifter can be localized to be recovered since its GPS position is sent immediately when it emerges.

2.4. Image processing for habitat evaluation

In this work, we will assess the state of the habitats using two different image classification methods:

(A) Images grabbed from the AUV were processed off-line, in the laboratory of the vessel, but just after the mission was completed. Photo-mosaics from each inspected area were built on a daily basis. Images occupy a position in the mosaic frame according to the camera global pose registered at the moment in which each image was captured, but scaled from meters to pixels thanks to the available navigation altitude. The camera global pose is computed by composing the output of the AUV navigation filter with the transform between the vehicle baselink and the camera lens (indistinctly left or right, depending on which images are used for the mosaic). Overlapping areas are then cropped and the color in them is homogenized with a Multi-Band blending strategy (Zhu et al., 2018). Photo-mosaics offer several benefits in this case: (1) a colored view of the whole area inspected by the AUV in a single image, (2) mosaics are geo-localized because the images were already geo-localized in the vehicle, offering a precise location and orientation in the earth map, (3) the possibility to perform a first visual and qualitative inspection and assessment of the seagrass distribution, (4) as the mission can be repeated with the AUV anytime in the same location and with the same regular or structured shape, mosaics of the same area build over successive seasons would give temporal series of data, useful to evaluate the progression of the inspected sites, (5) a single tool to compute the *Po* coverage rapidly, easily and accurately.

Coverage is computed following the next steps: (1) In order to discriminate the *Po* from the background, images forming the photo-mosaics were segmented with a pre-trained CNN model, from now on called *Posidonia Semantic Segmentation* (PSS) (Martin-Abadal et al., 2018). (2) Afterwards, the segmented images were used to build the same mosaic but in gray scale. (3) Thereafter, *Po* coverage can be easily calculated accounting for pixels of different gray scale levels. The main advantage with respect to the Line Intercept Transects strategy is that the calculation of the coverage is done in absolute terms rather than approximating or extrapolating linear measurements to surfaces.

PSS is supervised and uses a VGG16-FCN8 network architecture. It was trained on human-provided labeled annotations on a large set of images grabbed in diverse areas of the Balearics and Croatia, with different cameras, with many different textures and colors, different environmental conditions, in different seasons and different states of the seagrass, obtaining an accuracy over 87% (Martin-Abadal et al., 2018). The PSS already showed to provide excellent results when applied in preliminary field campaigns organized to mosaic and evaluate coastal areas of Mallorca colonized with *Po* (González et al., 2021). This trained model is already available for the community and presumably valid for the images taken in Cabrera, since its marine environment has, in general, many similarities with the environment of the rest of the Balearic islands.

(B) Raw underwater images gathered with the LD were also post-processed in the cruise laboratory in two phases: (1) color information was recovered with the open-source software suite *oplab_pipeline* (Massot-Campos et al., 2022) developed by the University of Southampton; the pipeline makes a gray world assumption and uses the altitude measurement to fit an attenuation curve per pixel to correct wavelength-dependent attenuation coefficients, and (2) in order to detect Po, images were also classified with a different trained CNN based on a mirrored AlexNet (Krizhevsky et al., 2017) structure, the *Location-Guided Autoencoder (LGA)* (Yamada et al., 2018). LGA has two principal characteristics, that make it more effective and adaptable than PSS: (1) it is an unsupervised feature learning method that does not require annotated datasets for training, and (2) it is capable of extracting information on ecological features that exist on spatial scales larger than the footprint of a single image.

Obtaining a reliable ground truth to compare the mosaics and the computed coverage is, at this moment, one of the major challenges in this type of applications. The public biological data available concerning location, extension and coverage of *Po* is either very limited, imprecise or directly non existent. The coverage results were compared with the coverage measures computed from a ground truth manually labeled on the color mosaics. The orientation and geo-localization of each mosaic was compared with the corresponding *habitat maps*, taking the border Po-sand as a valid reference. The accuracy in the extension and shape of each photo-mosaic is directly related with the programmed mission and the real trajectory performed by the robot, which is strongly conditioned by the accuracy of its navigation and localization modules, already demonstrated in previous work (Guerrero-Font et al., 2016; Font et al., 2017). In order to assess the performance of the LGA, a manually labeled ground truth was compared with the output of the network.

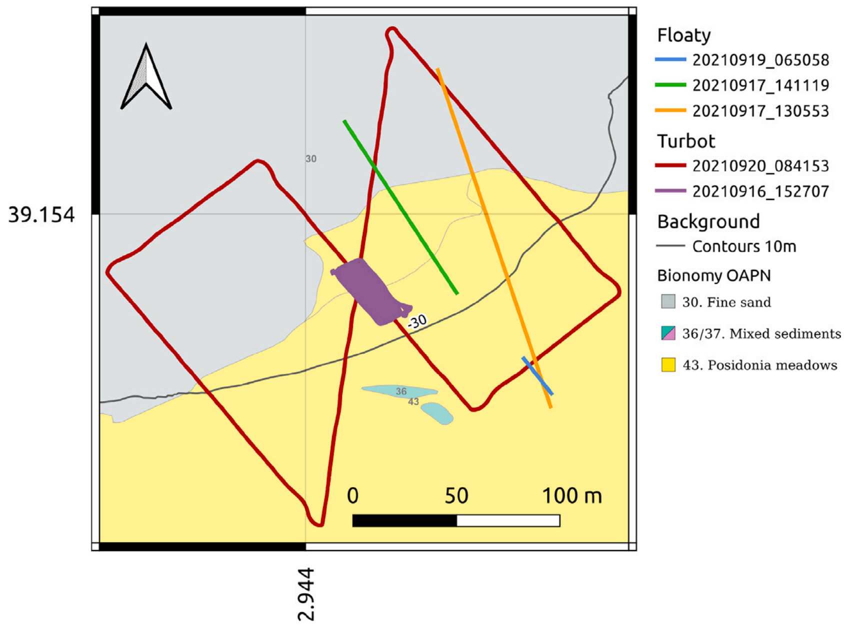

Fig. 4. Deployments of the marine platforms drawn on top of the known *habitat map*: (Organismo Autónomo Parques Nacionales, 2020) of Cabrera MPA.

Table 1
AUV-ASV mission times and descriptions.

Date	UTC start time	Duration (s)	# Images	Mission
15/09/2021	16:32:19	1944	3516	Dense survey
15/09/2021	18:18:30	2047	4121	Dense survey
16/09/2021	17:27:07	2947	5132	Dense survey
17/09/2021	11:28:39	3529	6953	Dense survey
17/09/2021	12:34:37	2765	5230	Sparse survey
18/09/2021	17:25:06	3767	7560	Sparse survey
20/09/2021	10:41:53	4295	8627	Sparse survey

Table 2
Drifter mission times and descriptions.

Date	UTC time	Duration (s)	# Images	Mission
16/09/2021	15:53:09	600	800	System check
17/09/2021	13:05:53	3600	1206	Drift
17/09/2021	14:11:19	3600	1151	Drift
18/09/2021	06:37:50	4200	3677	Drift
18/09/2021	14:45:02	3600	2358	Drift
20/09/2021	10:41:53	4295	8627	Drift

3. Field experiments

Two types of image datasets were obtained during the campaign. One type, which will be called from now on, dense and sparse surveys, were collected with the coordinated setup formed by the AUV and the ASV, and the other type will be called *drifts*, and executed with the Drifter.

The surveys performed by the AUV-ASV team were programmed to explore areas with *Po* meadows and sand transitions areas. These areas were selected because the *habitat map* of Cala Santa Maria is available and marked as colonized with Po, which means, a region of potentially rich ecosystems. The map shows important transitions between sand and Po, which evidence the lower limits of meadows and establish clear points of coincidence to be found between the habitat shape and the geo-referenced mosaics, in position and orientation. In any case, the evolution of the area is completely unknown, and the current state reflected in new mosaics can differ from the state of the site when the map was created. Let us consider this revision of the current map the other important result of this campaign.

Three types of missions were performed with the robots:

(a) Dense surveys with the AUV-ASV team: 40 × 20 m lawnmower-shaped trajectory with enough visual overlap across tracks of collected images; the objective is to generate a dense photo-mosaic of the covered area with no gaps.
(b) Sparse Surveys with the AUV-ASV team: 200 × 200 m lawn mower-shaped trajectory with no visual overlap across tracks; in this case, the objective is to cover areas larger than the ones covered with dense surveys, but establishing broader and sparser patterns of *Po*.
(c) Drifts: 30-minute-long drifts deployed in the working area to sparsely collect broader imagery.

Data gathering missions with the AUV-ASV team and LD are summarized in Table 1 and Table 2 respectively.

Fig. 4 shows some samples of the missions referred to before, plotted on top of the *habitat map*. All trajectories are Geo-localized in geodesic (latitude/longitude) coordinates.

Collectively, there were more than 20 h worth of data and more than 60.000 images over the six days when platforms were deployed. The longest mission with the AUV-ASV infrastructure is the last sparse survey with nearly 72 min, and the longest mission with the Drifter took also around 72 min. Fig. 5-(a)–(f) shows examples of images taken by the AUV during one of its missions, and Fig. 5-(g)–(h) shows one example of an image gathered with Floaty LD, color-corrected using Massot-Campos et al. (2022).

In this case, quality of all images is enough to discriminate the *Po* from the background, since the *Po* colonies seem to be settled on sandy bottoms, and the contrast is evident. The quality of images does not depend on the robotic platform but in the environmental conditions present during the missions.

3.1. Image mosaics

As mentioned in the previous section, the evaluation of the seagrass distribution in the areas surveyed with the AUV (see Table 1) was done with photo-mosaics.

Keyframes were extracted from the ROS-bag file of each AUV mission, each 0.35 meters of vehicle displacement, from its start to the end. Images were then debayerized, rectified using the known camera calibration parameters, downsampled by 4, color corrected and

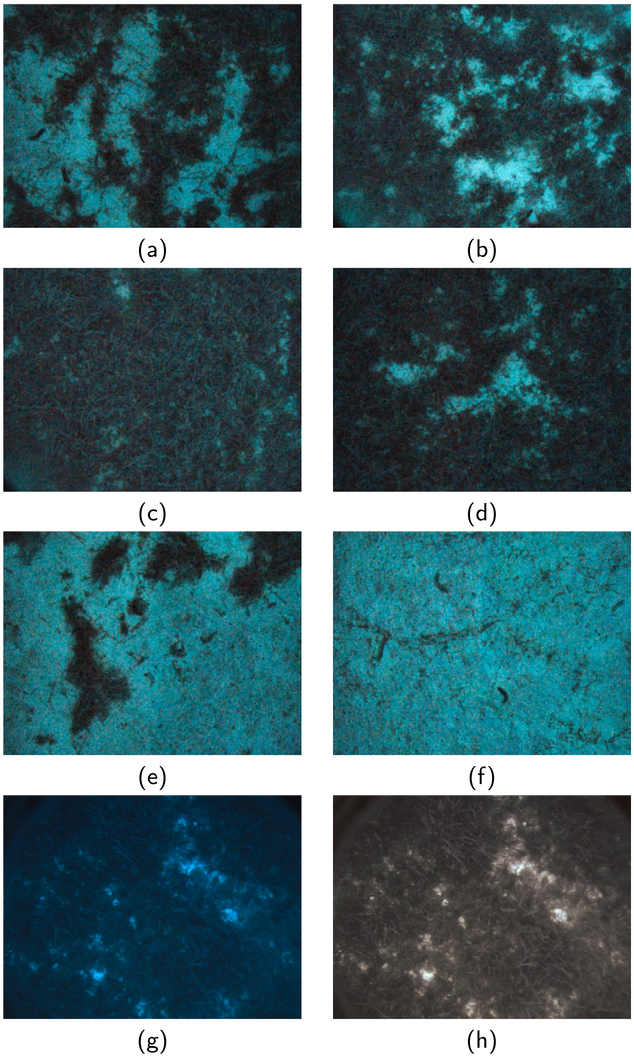

Fig. 5. (a) to (f) Examples of images taken from Turbot AUV.(g)–(h) Example of one image from Floaty LD, before and after color correction. (For interpretation of the references to color in this figure legend, the reader is referred to the web version of this article.)

contrast-enhanced using a CLAHE (Contrast Limited Adaptive Histogram Equalization) algorithm. In order to geo-reference the photo-mosaic, each key frame was related to its corresponding odometric camera global pose and the geodesic coordinates, both obtained at the precise moment of the image grabbing.

As two samples of datasets: Fig. 6-(a) shows the geo-referenced photo-mosaic built with 1260 keyframes extracted from the dense surveys of 16/09/2021, and Fig. 6-(b) shows the phot-mosaic built with 1300 keyframes extracted from the survey of 17/09/2021. Dark areas correspond to *Po* and clear areas correspond to sand. Figs. 7-(a) and 7-(b) show the corresponding odometric trajectories computed by the AUV localization module. Both mosaics share a common location and overlap in part of its extension. Note that the non-geo-referenced trajectories have a drift of 180° with respect to the geo-referenced mosaics. The boundary between sand and *Po* clearly visible in the photo-mosaic is part of the lower limit of the meadow, and, once geo-localized in the GIS system, a significant reference point to compare the old *habitat map* with the last datasets.

Results are presented in a Geo-localized information system (GIS) that shows the location of the mosaics in a geodesic (latitude/longitude) coordinate reference system (CRS).

3.2. *Po* semantic segmentation

The color images forming a certain photo-mosaic were input in the PSS trained model, but cropped and downsized to a resolution of 480 × 360 pixels. For each input color image, the network returns a gray scale output of size 480 × 360, where the gray level of each pixel indicates the probability of being *Po*. A value of zero means there is a 100% probability of it being Po, and a value of one is for a 0% probability. All gray-scale outputs were feather-blended using the same mosaic-building pipeline used to make the color mosaics, in order to generate the same geo-referenced mosaic but in gray scale. Before computing the coverage, the segmented mosaic must be binarized with a threshold that has to be set depending on the characteristics of the environment. In this case, the gray-level threshold was set to 75% since this is the value that offers the best trade-off between minimum *fall-out* and a maximum *recall* in our environment. Values used to compute *fall-outs* and *recalls* were referred to a ground truth, created on the original color mosaic but with the Po marked manually on it (González et al., 2021).

Finally, the *Po* bottom coverage was computed from the binarised mosaic as the percentage of pixels classified as *Po* with respect to the total amount of pixels of the mosaic. The resulting *Po* bottom coverage is 67.36% for the mosaic of 16/09/2021 and 68.32% for the mosaic of 17/09/2021, being the coverage measured from the hand-labeled ground truth 67.76% and 72.77%. However, this binarisation is sensitive to this threshold and so does the resulting coverage (González et al., 2021).

Figs. 8(a) and (b) show the resulting gray-level segmentation of the dense surveys performed on 16/09/2021 (a) and 17/09/2021 (b), superimposed on the original color mosaics. To ease identification, gray levels of segmentation have been swapped, being the *Po* overlaid in gray scale and sand in pure white.

3.3. Location-guided autoencoder

As a second habitat classification method, we present the results of the Location-Guided Autoencoder (LGA) (Yamada et al., 2018). LGA is an unsupervised convolutional neural network that can be trained with no human input. All images captured by the AUV and LD were used to train our LGA autoencoder for *Po* classification. The color input images were cropped and downsampled to a resolution of 227 × 227 pixels taking into account the camera calibration and the altitude they were taken at to homogenize the pixel size to a common metric. Data augmentations such as random rotations, random cropping and color noise were applied.

An additional procedure was added to the network training and testing: its resulting sixteen-dimensional inferred latent space was then hierarchically clustered and a very small subset with the 100 most representative training images were retrieved (Yamada et al., 2018). These subset was manually labeled to either be *Po* or background (sand). These labels were used to generate pseudo-labels in all the images. This information was then fed to the next step in the LGA algorithm, where a Support Vector Machine relabeled the rest of the latent space, and, consequently, the outputs. The results of this step applied to all the AUV and Drifter surveys of Fig. 4 can be seen in Fig. 9. The different probabilities of detecting *Po* are indicated in different shades of green, being, for instance, the green intensity level labeled as *seagrass_40_60* the corresponding to a positive probability between 40% and 60%.

There is certain difference between the limits between sand and *Po* visible in the *habitat map* and the limits that can be observed in the different datasets according to the LGA segmentation process. As shown in Fig. 9-(a), limits according to the *habitat map* are displaced to the north with respect to the limits marked by the dense survey and the southern part of the sparse survey. The limit between *Po* (different levels of green) and *other*, visible on the northern part of the sparse

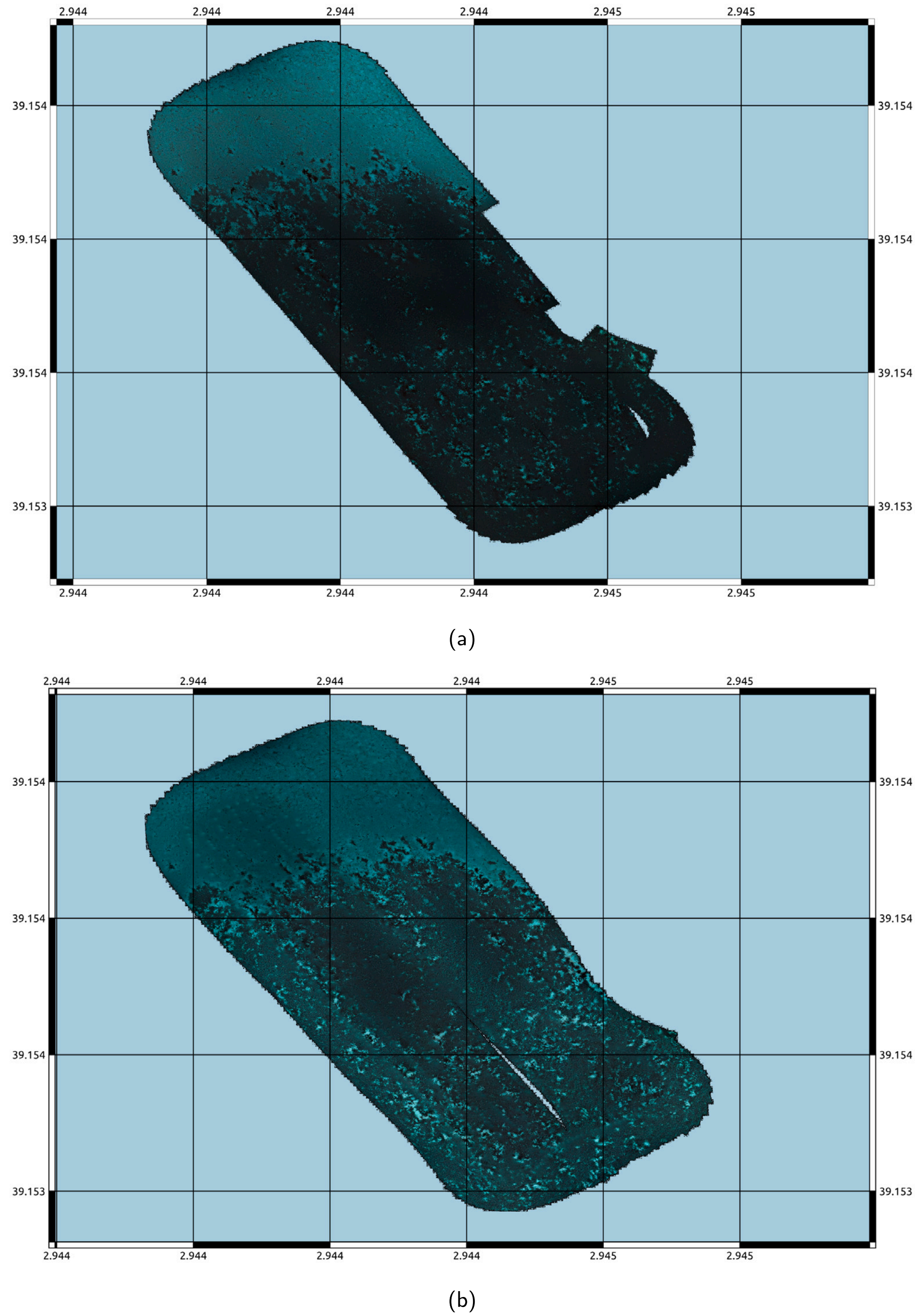

Fig. 6. Photo-mosaics corresponding to the dense surveys of 16/09/2021 in (a) and of 17/09/2021 in (b).

survey, coincides with the limits of the *habitat map*. The limits between *Po* and *other*, visible in the shortest drift are slightly moved to the north, but with a low detection probability after the border of the *habitat map*, while the classification in the longest drift still marks *Po* with certain probability inside the *sand* zone. This qualitative analysis suggests: (a) the limits of the *Po* meadow have displaced to the south, where the coast is located, meaning that, the meadow has regressed with respect to its previous state registered when the *habitat map* was made, and (b) the existence of several errors in the geo-localization and orientation of some datasets, being more evident in the longest drift. Errors in values of latitudes and longitudes can usually oscillate around a couple of meters, depending on the quality of the GPS device installed on the AUV and on the Drifter, but the possibility of a meadow regression is also highly plausible, given the global trend explained in the introduction.

Fig. 9-(b) shows, as an example, the LGA pseudo-labels output by LGA network on the images of the dense survey of 17/09/2021, superimposed on its colored mosaic. See as the zone marked with red level (Po) coincides, almost entirely, with the area of the mosaic covered with Po, marked in gray levels, in Fig. 8. It turns out that both segmentation trained models provide similar qualitative results about

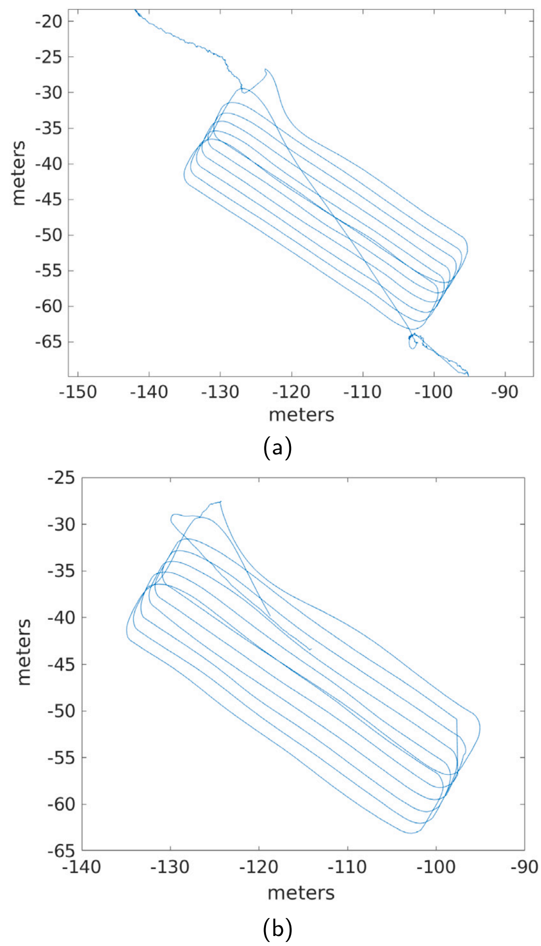

Fig. 7. Trajectories corresponding to the dense surveys done with Turbot AUV on 16/09/2021 in (a), and on 17/09/2021 in (b).

the presence or absence of Po, with the difference that LGA does not need entire supervision.

4. Discussion and conclusions

This paper has presented the objectives, workflows and results of the scientific cruise GRASSMAP, included in the Eurofleets European frame, planned as a proof of concept to use marine robots and advanced computer vision processing techniques to inspect and evaluate the state of seagrass meadows (Po) in certain areas of special ecological interest. The aim was to decrease risks and complexity of this type of missions, augment the amount and quality of field data, and increase accuracy of the post-processed information, compared to classical methods based on divers.

The main concern was to survey marine areas of the Cabrera National Park colonized with Po, at depths between 20 and 50 m, using two different autonomous robots, an AUV and a Lagrangian Drifter. ROVs and aerial drones with cameras were discarded due to costs, complexity and limitations in the type of missions that can be performed with the former, and the lack of detail that would have aerial images to be taken with the latter in the selected areas. Surveys were planned to grab video sequences close to the sea bottom and post-process them following specific workflows (mosaics + CNN segmentation + coverage computation) that permit to automatize the estimation of biological parameters related to the state of *Po* meadows, such as coverage or meadow boundaries. Our estimations can be qualitatively compared with the currently available *habitat map*; nevertheless, their accuracy and reliability were quantitatively assessed in previous work. In our campaigns, sending divers to the selected areas was completely unnecessary and, at these depths, absolutely discouraged, saving human costs, risks, and lessening complexity of missions. Data grabbed from divers at 40 meters would be rarely geo-localized with GPS, however, data obtained with our AUV is easily geo-referenced, because the GPS coordinates can be directly obtained once the robot is on the surface and composed with the odometry of the vehicle, corrected *in situ* by the USBL positioning.

Missions lasted a maximum of 70 min and covered, in dense surveys, approximately 800 m^2, in sparse surveys a maximum of 40000 m^2 and with Drifter, transects of 200 m, exceeding significantly the time a diver can be submersed at 40 meters depth and the extension of the sea bottom that can covered in a single immersion.

An important difficulty to evaluate our results, in terms of mosaic geo-localization and estimated *Po* coverage, was the lack of previous existing data. Figs. 8 and 9 show how the location of the different missions, either segmented with PSS or with LGA, coincide with the presence or absence of *Po* in the *habitat map*, and also, to a certain extent, with the boundary between *Po* and sand. The difference between the location of this boundary in the *habitat map* and in the dense and sparse geo-referenced mosaics suggests a regression of meadows and/or additional slight errors in the AUV geodesic measurements used to locate the images and the mosaics in the GIS system. Concerning the coverage estimations, its accuracy depends entirely on the accuracy of the mosaic and the performance of the trained CNN used for segmentation, which, in this case, are both highly adequate: the accuracy of the mosaic inherits the quality of the AUV localization (Font et al., 2017) system, while the excellent performance of the used CNN inference (Martin-Abadal et al., 2018) is necessarily reflected on the segmentation results. Combining multiple underwater images into a seamless mosaic has also shown in this work that large-area *Po* segmentation and coverage can be achieved without the need for human operators or divers, and that approximations or extrapolations can be substituted by the integration of global measurements. However, one of the requirements for mosaic-building is that images have enough overlap and that the seafloor in the area of interest is completely covered by the robot. This workflow is effective in dense surveys, but they require repetitive transects at short distance one from each other, augmenting considerably the time of the mission thus the amount of memory to store all data and images. Conversely, in sparse preprogrammed surveys, areas are partially covered, just to have a bare idea of the *Po* distribution and its morphology. Sparse missions can cover wider areas than dense, with the same time, but with much less details. Finally, the Drifter covered wide areas sparsely, following non-programmed trajectories with much less energy than AUVs, since they do not use thrusters to displace (only to submerse and emerge), offering a third alternative cheaper than the other two but with complementary results. Finding a trade off between planning dense or sparse surveys, or deploying the Drifter was another challenge of this campaign.

In summary, and similarly to previous approaches focused on other types of ecosystems, we got missions longer, deeper and more extensive than the ones performed by divers, with the desired shape and localization, more *in situ* data and better geo-localized, and coverage results more accurate than those estimated with the Line Intercept Transects strategy.

Presented workflows can be easily scalable to other mission shapes, lengths and depths, obviously taking into account limitations in the robot autonomy, computation resources and data storage capacity. Campaigns do not need to be restricted to the detection of *Po* but they can be focused on any other habitat feature, just retraining the

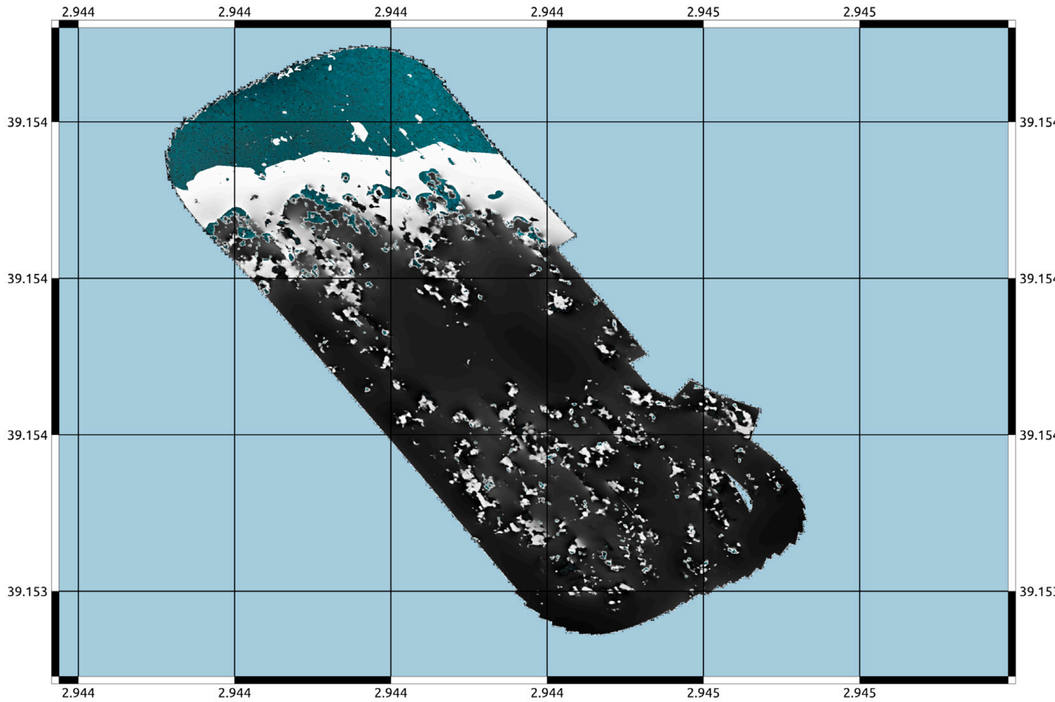

(a)

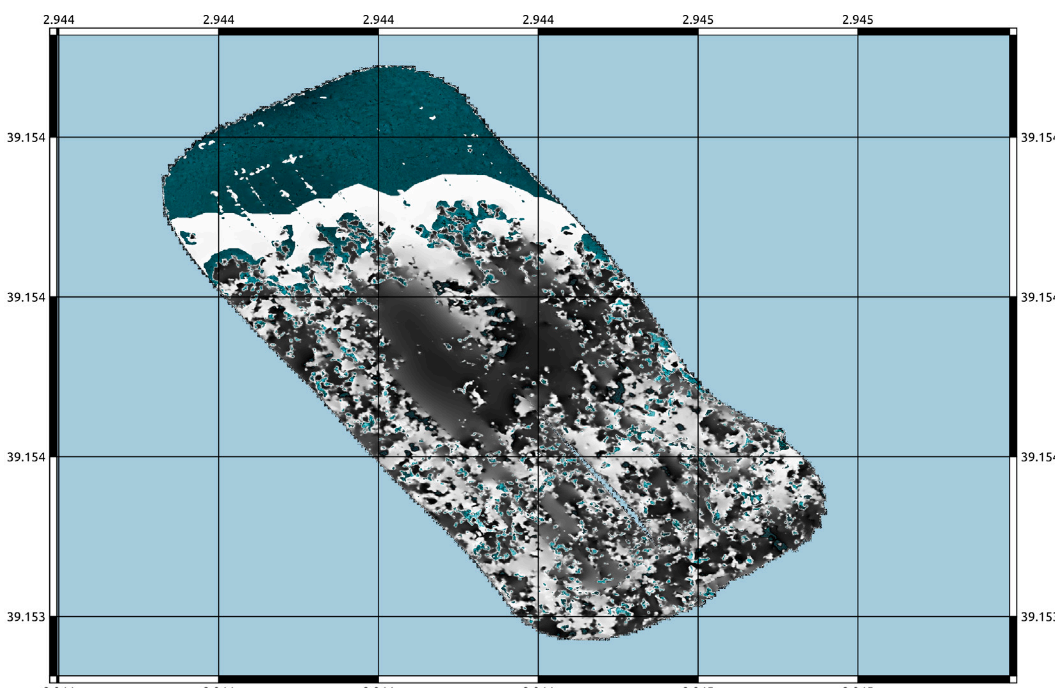

(b)

Fig. 8. Image segmentation using PSS method overlaid over the geo-localized mosaic.

CNNs and searching for reliable *ground truths* to validate against. In this particular campaign, missions were programmed to observe and map *Po* meadows at their deepest points (40–50 m), but, as explained in Yamada et al. (2018), LGA unsupervised training benefits from an unbiased feature representation, meaning that the second stage that classifies images in their latent representation can be tailored to other interest such as Essential Ocean Variables (EOVs) like fish, crustacea, corals or other types of seagrass or algae.

Future work intends to demonstrate the near-real-time awareness application on underwater vehicles, sending selected and critical information back to shore at any surfacing opportunity. This would enable operators to supervise the mission development and also to quickly understand what types of seafloor or habitats the robots have been monitoring up to that time. Applying this workflow to detect other EOVs for a better understanding of our oceans is also included in the ongoing and forthcoming work. In this campaign, we show

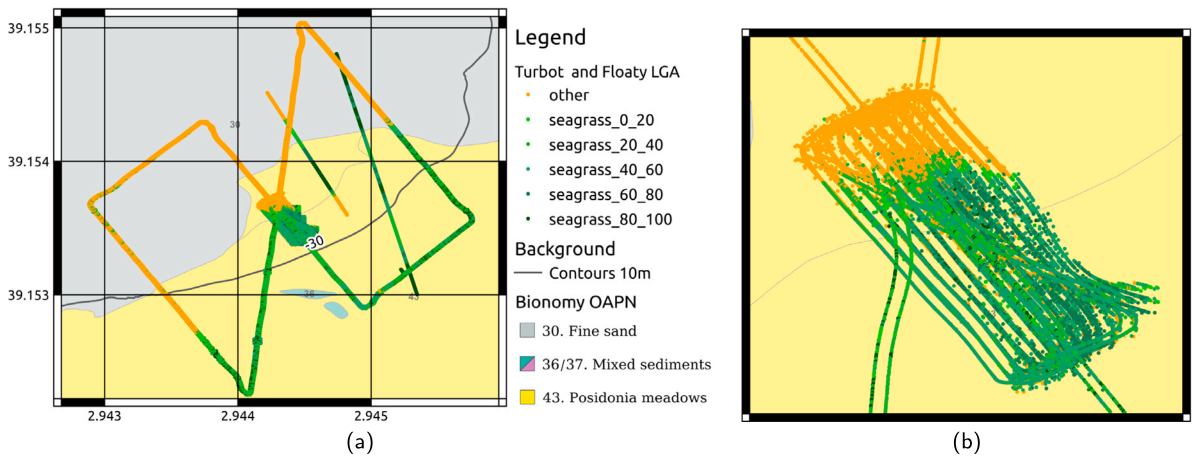

Fig. 9. (a) Classification of images using LGA, drawn in different levels of green, (b) Pseudo-labels on the dense survey trajectory.

how using AUV/Drifters for ecosystem monitoring is already state-of-the-art, and how science can shift towards marine robotics and science-enabled platforms rather than only robotics-driven research and manual extrapolations.

CRediT authorship contribution statement

Miquel Massot-Campos: Funding acquisition, Conceptualisation of this study, Methodology, Resources, Software, Project administration, Roles/Writing – original draft. **Francisco Bonin-Font:** Methodology, Software, Supervision, Validation, Writing – original draft. **Eric Guerrero-Font:** Data curation, Investigation, Methodology, Resources, Software. **Antoni Martorell-Torres:** Data curation, Investigation, Resources, Software. **Miguel Martin Abadal:** Data curation, Resources, Software. **Caterina Muntaner-Gonzalez:** Data curation, Resources, Software. **Bo Miquel Nordfeldt-Fiol:** Data curation, Resources, Software. **Gabriel Oliver-Codina:** Project administration, Supervision, Validation, Writing – review & editing. **Jose Cappelletto:** Resources, Software. **Blair Thornton:** Resources, Supervision, Writing – review & editing.

Declaration of competing interest

The authors declare no conflict of interest.

Data availability

Data is publicly available at https://www.emodnet-ingestion.eu/submissions/submissions_details.php?menu=39&tpd=1051&step_more=12_14_17&step=0821.

Acknowledgments

RV SOCIB ship-time was provided free of charge for the GRASSMAP survey, as part of the Eurofleets+ project which received funding from the European Union H2020 Research and Innovation Program under grant agreement No. 824077.

References

Abadie, A., Pace, M., Gobert, S., Borg, J.A., 2018. Seascape ecology in *Posidonia Oceanica* Seagrass Meadows: Linking structure and ecological processes for management. Ecol. Indic. 87, 1–13.
Baktash, E., Dehghani, M.J., Nasab, M.R.F., Karimi, M., 2015. Shallow water acoustic channel modeling based on analytical second-order statistics for moving transmitter/receiver. IEEE Trans. Signal Process. 63 (10), 2533–2545.
Balearic Islands Coastal Observing and Forecasting System, 2021. Research Vessel SOCIB. Available at https://www.socib.es/?seccion=vesselPage.
Barcelona, A., Colomer, J., Soler, M., Gracias, N., Serra, T., 2021. Meadow fragmentation influences *Posidonia Oceanica* density at the edge of nearby gaps. Estuar. Coast. Shelf Sci. 249, 107106.
Bonanno, G., Martino, V.D., 2017. Trace element compartmentation in the *Seagrass Posidonia Oceanica* and biomonitoring applications. Mar. Pollut. Bull. 116 (1), 196–203.
Bonin-Font, F., Burguera, A., Lisani, J.-L., 2017. Visual discrimination and large area mapping of *Posidonia Oceanica* using a lightweight AUV. IEEE Access 5, 24479–24494.
Bonin-Font, F., Lalucat, J., Oliver-Codina, G., Massot-Campos, M., Carrasco, P., 2018. Evaluating the impact of sewage discharges on the marine environment with a lightweight AUV. Mar. Pollut. Bull. 135, 714–722.
Campos, M.M., Codina, G.O., Bonin-Font, F., Font, E.G., Abadal, M.M., Fiol, B.M.N., Muntaner, C., 2021. GRASSMAP. Available at https://www.eurofleets.eu/classroom/#prettyPhoto[gallery_1]/66/ and at https://www.youtube.com/watch?v=jaIo1P1NFzQ.
Carreras, M., Hernández, J.D., Vidal, E., Palomeras, N., Ribas, D., Ridao, P., 2018. Sparus II AUV: A hovering vehicle for seabed inspection. IEEE J. Ocean. Eng. 43 (2), 344–355.
Deter, J., Lozupone, X., Inacio, A., Boissery, P., Holon, F., 2017. Boat anchoring pressure on coastal seabed: Quantification and bias estimation using AIS data. Mar. Pollut. Bull. 123 (1), 175–181.
DiCarlo, g., 2004. The Natural Recolonisation Process of the *Seagrass Posidonia Oceanica* (L.) Delile After the Introduction of the Italo-Algerian Methane Pipeline in the SW Mediterranean Sea (Ph.D. thesis). University of Southampton, Faculty of Engineering Science and Mathematics.
Duffy, J.P., Pratt, L., Anderson, K., Land, P.E., Shutler, J.D., 2018. Spatial assessment of intertidal seagrass meadows using optical imaging systems and a lightweight drone. Estuar. Coast. Shelf Sci. 200, 169–180.
European Commission, 2008a. Directive 2008/56/EC of the European Parliament and of the Council of 17 June 2008 Establishing a Framework for Community Action in the Field of Marine Environmental Policy. Available at https://www.eea.europa.eu/policy-documents/2008-56-ec.
European Commission, 2008b. MANAGEMENT of natura 2000 habitats. Posidonia Beds (*Posidonion oceanicae*). Available at https://ec.europa.eu/environment/nature/natura2000/management/habitats/pdf/1120_Posidonia_beds.pdf.
European Union’s Earth Observation Programme, 2021. Copernicus marine service. https://marine.copernicus.eu/.
Fabio, F.B.-M., Jimenez-Gutierrez, S., Martínez-Vidal, J., Guillén, J., Sánchez-Lizaso, J., 2022. Spatiotemporal trends observed in 20 years of *Posidonia Oceanica* monitoring along the Alicante Coast, Spain. Water 14 (3).
Fernández-Torquemada, Y., Díaz-Valdés, M., Izquierdo-Muñoz, A., Sánchez-Lizaso, J.L., Ramos-Esplá, A.A., 2020. Spatial and temporal variability of *Posidonia Oceanica* monitoring indicators, Valencian community, Spain. Water 12 (11).
Ferretti, R., Bibuli, M., Caccia, M., Chiarella, D., Odetti, A., Ranieri, A., Zereik, E., Bruzzone, G., 2017. Machine Learning Methods for Acoustic-based Posidonia Meadows detection by means of unmanned marine vehicles. In: OCEANS 2017 - Aberdeen. pp. 1–6.
Font, E.G., Bonin-Font, F., Carrasco, P.-L.N., Massot, M., Oliver, G., 2017. USBL integration and assessment in a multisensor navigation approach for AUVs. IFAC-PapersOnLine 50 (1), 7905–7910, 20th IFAC World Congress.
Gambi, M., Dappiano, M., Società Italiana di Biologia Marina, 2004. Mediterranean Marine Benthos: A Manual of Methods for Its Sampling and Study. SIBM.
GENCAT, 2022. Acció Climàtica. Available at http://agricultura.gencat.cat/ca/inici.
González, Y., Bonin-Font, F., Guerrero, E., Martorell, A., Martín, M., Oliver, G., 2021. Autonomous marine vehicles and CNN: Tech tools for posidonia meadows monitoring. In: IEEE Oceans.

Guerrero, E., Bonin-Font, F., Oliver, G., 2021. Adaptive visual information gathering for autonomous exploration of underwater environments. IEEE Access 9, 136487–136506.

Guerrero-Font, E., Bonin-Font, F., Martin-Abadal, M., Gonzalez-Cid, Y., Oliver-Codina, G., 2021. Sparse Gaussian process for online seagrass semantic mapping. Expert Syst. Appl. 170, 114478.

Guerrero-Font, E., Massot-Campos, M., Negre, P.L., Bonin-Font, F., Codina, G.O., 2016. An USBL-aided multisensor navigation system for field AUVs. In: 2016 IEEE International Conference on Multisensor Fusion and Integration for Intelligent Systems. MFI, pp. 430–435.

Gumusay, M.U., Bakirman, T., Kizilkaya, I.T., Aykut, N.O., 2019. A review of seagrass detection, mapping and monitoring applications using acoustic systems. Eur. J. Remote Sens. 52 (1), 1–29.

Hong, S., Chung, D., Kim, J., 2017. Development of a Hover-capable AUV system for automated visual ship-hull inspection and mapping. In: OCEANS 2017 - Anchorage. pp. 1–5.

IQUA ROBOTICS, 2022. IQUA ROBOTICS. Available at https://iquarobotics.com.

Kiparissis, S., Fakiris, E., Papatheodorou, G., Geraga, M., Kornaros, M., Kapareliotis, A., Ferentinos, G., 2011. Illegal trawling and induced invasive algal spread as collaborative factors in a *Posidonia Oceanica* meadow degradation. Biol. Invasions 13 (3), 669–678.

Krizhevsky, A., Sutskever, I., Hinton, G.E., 2017. ImageNet classification with deep convolutional neural networks. Commun. ACM 60 (6), 84–90.

Lambertini, A., Menghini, M., Cimini, J., Odetti, A., Bruzzone, G., Bibuli, M., Mandanici, E., Vittuari, L., Castaldi, P., Caccia, M., De Marchi, L., 2021. Monitoring and surveying from an underwater vehicle in SUSHI DROP project. In: 2021 International Workshop on Metrology for the Sea; Learning to Measure Sea Health Parameters (MetroSea). pp. 189–193.

Lemenkova, P., 2011. Seagrass Mapping and Monitoring Along the Coast of Crete, Greece (Master's thesis). University of Twente.

Louchard, E., Reid, R., Stephens, F., Davis, C., Leathers, R., Downes, T., 2003. Optical remote sensing of benthic habitats and bathymetry in coastal environments at Lee Stocking Island, Bahamas: A comparative spectral classification approach. Limnol. Oceanogr. 48, 511–521.

Marbà, N., Duarte, C., 1998. Rhizome elongation and seagrass clonal growth. Mar. Ecol. Prog. Ser. 174.

Marbà, N., Duarte, C., 2010. Mediterranean warming triggers seagrass (*Posidonia Oceanica*) shoot mortality. Global Change Biol. 16 (8).

Marbà, N., Duarte, C., Holmer, M., Martínez, R., Basterretxea, G., Orfila, A., Tintoré, J., 2002. Effectiveness of protection of seagrass (*Posidonia Oceanica*) populations in cabrera national park (Spain). Environ. Conserv. 29 (4), 509–518.

Martin-Abadal, M., Guerrero-Font, E., Bonin-Font, F., González-Cid, Y., 2018. Deep semantic segmentation in an AUV for online *Posidonia Oceanica* meadows identification. IEEE Access 6 (1), 60956–60967.

Martorell-Torres, A., Massot-Campos, M., Guerrero-Font, E., Oliver-Codina., G., 2018. Xiroi ASV: A modular autonomous surface vehicle to link communications. In: IFAC-PapersOnLine. 51, (29), pp. 147–152.

Massot-Campos, M., Bodenmann, A., Thornton, B., 2022. Ocean perception laboratory pipeline (oplab_pipeline)- version= 1.0.0. Available at https://github.com/ocean-perception/oplab_pipeline.

McKenzie, L., 2003. Guidelines for the Rapid Assessment of Seagrass Habitats in the Western Pacific. In: QFS, NFC, Caims, Seagrass-Watch HQ, PO Box 6811, Caims, QLD, 4870 Australia.

McLean, D.L., Parsons, M.J.G., Gates, A.R., Benfield, M.C., Bond, T., Booth, D.J., Bunce, M., Fowler, A.M., Harvey, E.S., Macreadie, P.I., Pattiaratchi, C.B., Rouse, S., Partridge, J.C., Thomson, P.G., Todd, V.L.G., Jones, D.O.B., 2020. Enhancing the scientific value of industry remotely operated vehicles (ROVs) in our oceans. Front. Mar. Sci. 7.

Mizuno, K., Terayama, K., Tabeta, S., Sakamoto, S., Matsumoto, Y., Sugimoto, Y., Ogawa, T., Sugimoto, K., Fukami, H., Sakagami, M., Deki, M., Kawakubo, A., 2020. Development of an efficient coral-coverage estimation method using a towed optical camera array system [speedy sea scanner (SSS)] and deep-learning-based segmentation: A sea trial at the Kujuku-Shima Islands. IEEE J. Ocean. Eng. 45 (4), 1386–1395.

Ocean Scan Marine Systems and Technology Lda, 2022. Light underwater autonomous vehicle. Available at https://www.oceanscan-mst.com/.

Organismo Autónomo Parques Nacionales, 2020. Bionomía y Batimetría de los Fondos Marinos de los Parques Nacionales Marítimo-Terrestres Españoles (Spanish Ministry for the Ecological Transition and the Demographic Challenge). Available at https://datos.gob.es/es/catalogo/ea0022425-seguimientomediomarino.

Perkins, N.R., Foster, S.D., Hill, N.A., Barrett, N.S., 2016. Image subsampling and point scoring approaches for large-scale marine benthic monitoring programs. Estuar. Coast. Shelf Sci. 176, 36–46.

Perkins, N., Hill, N., Foster, S., Barrett, N., 2015. Altered Niche of an ecologically significant urchin species, Centrostephanus Rodgersii, in its extended range revealed using an autonomous underwater vehicle. Estuar. Coast. Shelf Sci. 155, 56–65.

Piñeiro-Juncal, N., Kaal, J., Moreira, J.C.F., Cortizas, A.M., Lambais, M.R., Otero, X.L., Mateo, M.A., 2021. Cover loss in a *Seagrass Posidonia Oceanica* Meadow accelerates soil organic matter turnover and alters soil prokaryotic communities. Org. Geochem. 151, 104140.

Rende, S.F., Bosman, A., Di Mento, R., Bruno, F., Lagudi, A., Irving, A.D., Dattola, L., Giambattista, L.D., Lanera, P., Proietti, R., Parlagreco, L., Stroobant, M., Cellini, E., 2020. Ultra-high-resolution mapping of *Posidonia Oceanica* (L.) delile meadows through acoustic, optical data and object-based image classification. J. Mar. Sci. Eng. 8 (9).

Risio, M.D., D'Ovidio, G., Celli, D., Pasquali, D., 2018. Underwater remotely operated vehicles for fast and low cost bathymetry surveys. In: 2018 IEEE International Workshop on Metrology for the Sea; Learning To Measure Sea Health Parameters. MetroSea, pp. 23–27.

Sgorbini, S., Peirano, A., Cocito, S., Morgigni, M., 2002. An underwater tracking system for mapping marine communities: An application to *Posidonia Oceanica*. Oceanol. Acta 25, 135–138.

Stanford Artificial Intelligence Laboratory, et al., 2021. Robotic operating system. https://www.ros.org, ROS Melodic Morenia.

Sylvie, G., Stephane, S., Valerie, R.-R., Bruno, A., Aurelia, C., Pierre, L., Pierre, B., 2009. Assessment of the ecological status of Mediterranean French Coastal waters as required by the water framework directive using the *Posidonia Oceanica* Rapid Easy Index: PREI. Mar. Pollut. Bull. 58 (11), 1727–1733.

Thornton, B., Bodenmann, A., Yamada, T., Stanley, D., Massot-Campos, M., Huvenne, V., Durden, J., Bett, B., Ruhl, H., Newborough, D., 2021. Visualizing multi-hectare seafloor habitats with BioCam. Oceanography.

UIB, IMEDEA, 2022. DETECPOS: DEvelopment of new TEChnologies for the Automatic and Periodic Assessment of Changes in POSidonia Meadows due to Anthropogenic Causes. Available at http://srv.uib.es/detecpos/.

Vasilijevic, A., Miskovic, N., Vukić, Z., Mandić, F., 2014. Monitoring of Seagrass by Lightweight AUV: A *Posidonia Oceanica* case Study surrounding Murter Island of Croatia. In: 2014 22nd Mediterranean Conference on Control and Automation. MED 2014.

Ventura, D., Bonifazi, A., Gravina, M.F., Belluscio, A., Ardizzone, G., 2018. Mapping and classification of ecologically sensitive marine habitats using unmanned aerial vehicle (UAV) imagery and object-based image analysis (OBIA). Remote Sens. 10 (9).

Verfuss, U.K., Aniceto, A.S., Harris, D.V., Gillespie, D., Fielding, S., Jiménez, G., Johnston, P., Sinclair, R.R., Sivertsen, A., Solbø, S.A., Storvold, R., Biuw, M., Wyatt, R., 2019. A review of unmanned vehicles for the detection and monitoring of Marine Fauna. Mar. Pollut. Bull. 140, 17–29.

Wenzhoefer, F., Wulff, T., Floegel, S., Sommer, S., Waldmann, C., 2016. ROBEX - innovative robotic technologies for ocean observations, a deep-sea demonstration mission. In: OCEANS 2016 MTS/IEEE Monterey. pp. 1–8.

Williams, S.B., Pizarro, O.R., Jakuba, M.V., Johnson, C.R., Barrett, N.S., Babcock, R.C., Kendrick, G.A., Steinberg, P.D., Heyward, A.J., Doherty, P.J., Mahon, I., Johnson-Roberson, M., Steinberg, D., Friedman, A., 2012. Monitoring of benthic reference sites: Using an autonomous underwater vehicle. IEEE Robot. Autom. Mag. 19 (1), 73–84.

Yamada, T., Prügel-Bennett, A., Thornton, B., 2018. Learning features from georeferenced seafloor imagery with location guided autoencoders. J. Field Robotics 38, 52–67.

Yang, Q., Massot-Campos, M., Das, S.K., Thornton, B., Pizarro, O., 2020. Deployment strategies for representative surveys using passive drifting seafloor imaging floats. In: Proc. IEEE/OES Autonomous Underwater Vehicles Symposium. AUV, pp. 1–6.

Zhu, Z., Lu, J., Wang, M., Zhang, S., Martin, R.R., Liu, H., Hu, S.-M., 2018. A comparative study of algorithms for realtime panoramic video blending. IEEE Trans. Image Process. 27 (6), 2952–2965.

Zoffoli, M.L., Frouin, R., Kampel, M., 2014. Water column correction for coral reef studies by remote sensing. Sensors 14 (9), 16881–16931.